九州大学学術情報リポジトリ
Kyushu University Institutional Repository

Label-Free Cancer Stem-like Cell Assay Conducted at a Single Cell Level Using Microfluidic Mechanotyping Devices

Terada, Miyu
Department of Applied Chemistry, Graduate School of Engineering, Kyushu University

Ide, Sachiko
Department of Applied Chemistry, Graduate School of Engineering, Kyushu University

Naito, Toyohiro
Department of Applied Chemistry, Graduate School of Engineering, Kyushu University

Kimura, Niko
Department of Applied Chemistry, Graduate School of Engineering, Kyushu University

他

https://hdl.handle.net/2324/7160842

出版情報：Analytical Chemistry. 93 (43), pp.14409-14416, 2021-10-09. American Chemical Society
バージョン：
権利関係：

KYUSHU UNIVERSITY

Label-free cancer stem-like cell assay conducted at a single cell level using microfluidic mechanotyping devices

Miyu Terada[†], Sachiko Ide[†], Toyohiro Naito[†], Niko Kimura[†], Michiya Matsusaki[‡], Noritada Kaji[†*]

[†]Department of Applied Chemistry, Graduate School of Engineering, Kyushu University, 744 Motooka, Nishi-ku, Fukuoka 819-0395, Japan

[‡]Department of Applied Chemistry, Graduate School of Engineering, Osaka University, 2-1 Yamadaoka, Suita, Osaka 565-0871, Japan

ABSTRACT: The mechanical phenotype of cells is an intrinsic property of individual cells. In fact, this property could serve as a label-free, non-destructive, diagnostic marker of the state of cells owing to its remarkable translational potential. A microfluidic device is a strong candidate for meeting the demand of this translational research as it can be used to diagnose a large population of cells at a single cell level in a high-throughput manner, without the need for off-line pretreatment operations. In this study, we investigated the mechanical phenotype of the human colon adenocarcinoma cell, HT29, which is known to be a heterogeneous cell line with both multipotency and self-renewal abilities. This type of cancer stem-like cells (CSCs) is believed to be the unique originators of all tumor cells and may serve as the leading cause of cancer metastasis and drug resistance. By combining consecutive constrictions and microchannels with an ionic current sensing system, we found a high heterogeneity of cell deformability in the population of HT29 cells. Moreover, based on the level of aldehyde dehydrogenase (ALDH) activity and the expression level of CD44s, which are biochemical markers that suggest the multipotency of cells, the high heterogeneity of cell deformability was concluded to be a potential mechanical marker of CSCs. The development of label-free and non-destructive identification and collection techniques for CSCs has remarkable potential not only for cancer diagnosis and prognosis, but for the discovery of a new treatment for cancer.

The mechanical properties of cells are valuable indicators of changes in the internal structure of cells as they reflect both the state and function of cells. The mechanical properties of cells have also been recognized as a new label-free biomarker that is comparable to existing biochemical biomarkers. As a result, these properties have remarkable translational potential[1]. Alterations in the mechanical properties of cells have been linked to processes, such as cell cycle progression[2], cancer malignancy[3,4], stem cell differentiation[5–8], and leukocyte activation[9,10]. To date, various types of single cell mechanotyping techniques have been developed, such as micropipette aspiration[11], filtration[12,13], optical tweezers[14], atomic force microscopy (AFM)[15], microplate manipulation[16], and magnetic tweezers[17]. These methods evaluate time-resolved responses to force and enable the extraction of physical properties, such as elastic modulus or viscosity. However, these techniques are limiting as they are technically demanding and time-consuming, which limit measurement throughput and their use beyond specialized laboratories. Obtaining quantitative and reliable measurements of mechanical properties from a large population of cells has always been a challenge. More recently, characterizing the mechanical properties of over tens to hundreds of individual cells per second in inherently heterogeneous cell populations using microfluidic devices has become an important and useful strategy in cell biology due to the simplicity, label-free, low-cost, non-destructive, and high-throughput features of these devices. These approaches have remarkable potential for implementation in both biological laboratories and clinical settings[18].

In combination with several biophysical markers, such as relative nuclear fluctuation, cell spread area, and nucleus-to-cytoplasm ratio, cell deformability was demonstrated to be predictive of the multipotency of human mesenchymal stromal cells (hMSCs) *in vivo* as well as after *in vitro* expansion[19]. The expression of over 48,000 human transcripts were investigated and the differential expression of osteogenic genes as well as genes associated with the maintenance of a stem cell program in hMSCs was revealed. Moreover, pluripotency in mice neural lineage was evaluated by mechanotyping during reprograming to induced pluripotent stem cells (iPSCs) and differentiation to the original feral neural progenitor cells (fNPCs)[6]. By using qRT-PCR, researchers confirmed the upregulation of pluripotency genes, such as *Nanog* and *E-cadherin* (*Ecad;* or *Cdh1*), and the downregulation of neural markers expressed in fNPCs, such as *Sox1* and *Vimentin (Vim)*. In addition, the expression of two surface markers, SSEA1 (an early pluripotency marker) and CD24 (an indicator used to identify doxycycline-dependent F-class cells), were simultaneously monitored. These two approaches are typical examples of a challenge in noninvasive single cell analysis as there are biochemical, molecular, and structural features underlying the mechanical differences.

In fact, not limited to stem cell research, cancer stem-like cells (CSCs) are currently recognized as unique originators of all tumor cells and preside the tumor growth as the top of the cellular hierarchy. CSCs are considerably more plastic than

originally expected, thereby making therapy more difficult. In 1994, a human acute myeloid leukemia (AML)-initiating cell was identified through a study carried out with severe combined immune deficient (SCID) mice. This *in vivo* model experiment revealed a new leukemia-initiating cell based on cell surface marker expression (i.e., CD34-positive and CD38-negative)[20,21]. Thereafter, these CSCs were found in solid tumors, such as breast[22], prostate[23], pancreatic[24], colon[25], and ovarian cancers[26], and identified based on the expression level of CD44 and CD133. CD44s, the conventional isoform of CD44, is a cell-surface glycoprotein controlling cell-cell adhesion and migration. In some epithelial cancer cells, variant isoforms of CD44 are closely connected to cancer metastasis and invasion[27]. Especially in the gastrointestinal system, resistance to reactive oxygen species (ROS) is a specific marker distinguishing cellular stemness[28,29]. The clinical research explored that the variant isoforms of CD44 is highly specific to the type of cancer, for example, CD44v6 is not related to cholangiocarcinoma (CCA) progression while CD44v9 has a strong relevance to the CCA[27,30,31]. Another biochemical marker of CSCs, aldehyde dehydrogenase (ALDH), an intracellular enzyme involves in cellular detoxification, differentiation, and drug resistance[32,33]. ALDH1 is known as a CSC marker in breast cancer as well as CCA, where its high expression suggested poor prognosis in the patients. In the CCA cell line, TFK-1, the mesenchymal properties have been demonstrated based on ALDH1 expression level. In fact, several markers including ALDH have been used to identify CSCs in various types of cancers; the frequency is suggested to be <1 CSC per 1,000 cancer cells.

In this study, we investigated the mechanical properties of HT29 cells, which is known to be a heterogenous cell line possessing both multipotency and self-renewal abilities[34–36], using microfluidic devices, biochemical markers of CD44 and CD133 expression, and ALDH activity. Previously, we developed a method to measure cell deformability, which enabled us to successfully assess the cell cycle[37] and detect circulating cancer cells (CTCs) in whole blood[38]. To measure cell deformability, we first examined the width of the rear constriction by using the current measurement method and a microfluidic device. Thereafter, we evaluated the deformability of HT29 (human colon adenocarcinoma), Caco-2 (human colon adenocarcinoma), HeLa (human cervical cancer), MDA-MB-231 (human mammary carcinoma), and Jurkat (human leukemia T cells) cells. We also evaluated the multipotency of HT29 cells using a conventional method of CSCs evaluation, which is based on the level of CD44v9 expression and ALDH activity. In combination with the biochemical assay results, mechanotyping was revealed to be a powerful technique for identifying CSCs in a label-free and non-invasive manner.

MATERIAL AND METHODS

Device fabrication. In fabrication of polydimethylsiloxane (PDMS)-based microfluidic devices, standard soft lithography methods were used. Masks for photolithography to pattern the microfluidic channel design on a mask blank (CBL4009BuAZP, Clean Surface Technology Co., Kanagawa, Japan) were fabricated using a maskless lithography system (D-light DL-1000GS/NC, Nanosystem Solutions, Inc., Tokyo, Japan). A negative photoresist, SU-8 3025 (Nippon Kayaku Co. Ltd., Tokyo, Japan), was coated at 20 μm thick onto a silicon wafer by a spin coater (1H-DXII, Mikasa Co., Ltd., Tokyo, Japan) and the wafer was baked for 10 min at 95 °C as a prebake process. The photoresist was exposed to UV through the designed mask using a standard lithography mask aligner (MA-10, Mikasa Co., Ltd., Tokyo, Japan) and then post baked for 3 min at 95 °C. The UV exposed pattern was developed by an SU-8 developer (Nippon Kayaku Co., Ltd., Tokyo, Japan) and washed with 2-propanol (Wako Pure Chemical Industries, Ltd., Tokyo, Japan) to remove the uncured photoresist. The fabricated master mold was silanized in vapor of trichloro(1H,1H,2H,2H-perfluorooctyl)silane (Sigma-Aldrich Co. LLC., Tokyo, Japan), and then, a mixture of a PDMS curing agent and PDMS prepolymer (SYLGARD 184 Silicone Elastomer Kit, Dow Corning Toray Co., Ltd., Tokyo, Japan) was poured into the master mold in a 1:10 weight ratio. The pre-cured PDMS device was degassed in a vacuum desiccator for 1 h and subsequently cured for 12 h at 65 °C. The cured PDMS replica was carefully peeled from the master mold and reservoirs were punched for the tubing connected to a syringe pump and electrodes. The surface of the PDMS replica was treated with a soft plasma etching (SEDE-PFA, Meiwafosis Co., Ltd., Tokyo, Japan) for 90 s at 5 mA and then bonded with a slide glass for 1 min at 180 °C. In prior to bonding, selected areas of the slide glass were manually masked with adhesive polyimide tape (Kapton® tape, Thorlabs, Inc., NJ) and 40-nm thick of gold electrodes were deposited onto the slide glass by rf magnetron sputtering (MSP-mini, Vacuum Device, Co., Ltd., Mito, Japan).

Cell Culture. All reagents used for cell culture were purchased from FUJIFILM Wako Pure Chemical Corporation, unless otherwise stated. HT20 cells (a human colon adenocarcinoma cell line) and Jurkat cells (a human T-cell lymphoma cell line) were cultured in Roswell Park Memorial Institute 1640 Medium (RPMI-1640 with L-Glutamine and Phenol Red) at 37 °C in 5% CO_2. HeLa cells (a human cervical carcinoma cell line) were cultured under the same conditions in Eagle's Minimal Essential Medium (E-MEM with L-Glutamine and Phenol Red) supplemented with a 1% penicillin/streptomycin antibiotic mixture. Caco-2 (a human Colon adenocarcinoma cell line) and MDA-MB231 (a breast tumor cell line) cells were cultured under the same conditions in Dulbecco's Modified Eagle's Medium−high glucose (D-MEM (High Glucose) with L-Glutamine and Phenol Red). All media were supplemented with heat-inactivated 10% fetal bovine serum (FBS, 10270106, Thermo Fisher Scientific K.K., Tokyo, Japan). HeLa and MDA-MB-231 cells were cultured in 25 cm^3 culture flasks at near-confluent and were treated with trypsin solution (0.5 w/v% Trypsin-5.3 mmol/L EDTA・4 Na Solution without Phenol Red) for 3 min to detach from the flasks. The suspended cells were collected in a 15 mL conical tube. After centrifugation at 4 °C for 3 min at 1000 rpm, the cell pellets were collected and resuspended in the culture medium at an adequate concentration for either subculture or the subsequent mechanotyping experiments. HT29 and Caco-2 cells were treated using the same conditions as above, except that the treatment time with trypsin was 5 min for both the cells. The Jurkat cells were cultured and treated via the same conditions used for HT29 cells except for trypsin treatment. The cell sizes were measured in a suspended state immediately after trypsin treatment by capturing the images using a microscope (ECLIPSE Ts2, Nikon, Tokyo,

Japan) and an image analysis software (ToupView, Toup Tek Photonics, Zhejiang, P.R. China).

Evaluation of Cell Deformability via Ionic Current Measurement. The simultaneous detection system consisting of an ionic current and microscopic observation was originally developed in our group; the detail setup of this system is described elsewhere[37–42]. The microfluidic channels were connected to components through silver wires and the whole electrical circuit is depicted in Figure 1. Prior to the electrophoresis and the ionic current measurements, the variable-resistance element in the detection circuit was adjusted to 0 A and prevented current flow into the detection circuit. When a cell passes through the constrictions, the resistance in the constrictions increase and the current bypasses the series of detection channel through the detection circuit. Of note, the experiments assured that the current intensity and its duration time are proportional to the cell volume and resident time in the constrictions, respectively. The *p* values obtained by comparing the normalized residence time were calculated by Tukey (HSD: honestly significant difference) test using KaleidaGraph 4.5 (HULINKS, Inc., Tokyo, Japan). A constant current around a few hundred nA to μA level flows in a conventional series circuit and generates Joule heating which disrupts ion migration especially in the relatively high ionic strength and conductivity buffer (~1.6 S/m). As illustrated in Figure 1D, the bridge circuit can reduce this thermal fluctuation leading to the high background noise because the electrophoretic current detours to the ampere meter on the bridge circuit when there is no sample in the detection area. When the sample enters into the detection area, the corresponding electrophoretic current detours to the bridge circuit and detected by the ampere meter as illustrated in Figure 1D(i) and 1D(iii). As a result, the background noise is markedly decreased without any loss in signal intensity and response time. For this cell measurement, electrophoretic force alone was insufficient to draw cells into the constrictions; therefore, a syringe pump (KDS200, KD Scientific, Holliston, MA) was connected to a reservoir through a silicone tube, as illustrated in Figure 1A, and hydrodynamically withdrew the cells to assist the electrophoretic move. Buffer conductivity was measured using a benchtop conductivity meter (DS-52, Horiba, Ltd., Kyoto, Japan) and the obtained value was subsequently used to calculate the diameters of cells (Table S1). The device connected to the electrical circuit was placed on an inverted microscope (Eclipse Ti, Nikon, Tokyo, Japan) and the detection area was directly observed during the ionic current measurement, if necessary.

ALDH activity assay. To evaluate the multipotency of cancer cells, the ALDH activities of HT29, Caco-2, HeLa, and MDA-MB-231 cells were measured using the AldeRed™ ALDH Detection Assay kit (SCR150, Merk-Millipore, Tokyo, Japan). A suspension of the cultured cells was dispensed into each 1.5 mL microtube and the supernatant was removed by centrifugation at 250 ×g for 5 min at 4 °C. Thereafter, we added 1 mL of ALDH activity assay buffer and Verapamil to the two microtubes containing cell pellet prior to agitation. Five μL of an inhibitor of ALDH activity, N,N-diethylaminobenzaldehyde (DEAB), was added to only one tube and another tube was used as the control sample; the two tubes were incubated for 30 min at 37 °C. All tubes were centrifuged at 250 ×g for 5 min at 4 °C and the supernatant was discarded. After the addition of 500 μL of ALDH activity assay buffer and Verapamil, the samples were stored on ice

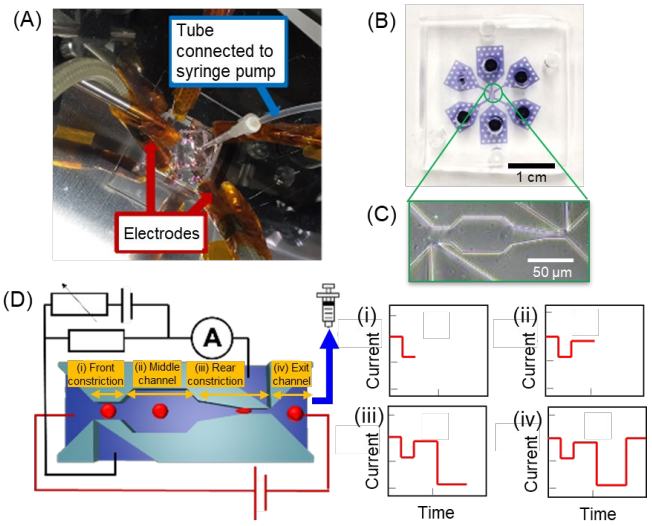

Figure 1. Overview of the experimental setup of the mechanical phenotyping device. (A) Image of the mechanical phenotyping device composed of PDMS microfluidic channels, a glass slide, four electrodes, and a silicone tube. (B) Image of the PDMS device. The channels and the reservoirs are filled with colored water for easier observation. (C) Microscopic image of the consecutive constrictions and channels. (D) The detection scheme in the mechanical phenotyping device. When a cell migrates from the front constriction to the exit channel, the electrical signals depicted from (i) to (iv) are obtained.

under dark conditions until the performance of the ALDH assay.

HT29 cells and HeLa cells were analyzed by flow cytometry (CytoFLEX S, Beckman Coulter) while Caco-2 and MDA-MB-231 cells were analyzed using a cell sorter (SH800, SONY, Tokyo, Japan). To prevent cell aggregation, a FALCON® cell strainer was used to disperse the cells before measurement.

CD44v9 assay. The assay was performed according to the methods provided by the company. The cell suspension prepared using approximately 6×10^6 cell/mL was transferred to 1.5 mL microcentrifugation tubes and centrifuged at 250 ×g for 5 min at 4 °C to remove the supernatant. In addition, 1 mL of 2% FBS in PBS was added to each tube, and the tubes were kept on ice for 15 min to prevent non-specific adsorption of the antibodies. After the blocking, step the tubes were centrifuged at 250 ×g for 5 min at 4 °C and the supernatant was removed. Three mL of the primary antibody, Anti-Human CD44v9 (LKG-M003, Cosmo Bio Co., Ltd., Tokyo, Japan; diluted 300-fold in PBS with 2% FBS) was added to the tube containing cells and mixed well. The mixture was kept at 4 ˚C under dark conditions for 45 min. After the reaction, the cells were washed three times with 1 mL of PBS by centrifugation. For the secondary antibody reaction, 30 µL of APC-H7 Mouse Anti-Human CD44 (56532, BD Biosciences, San Jose, CA; diluted 20-fold in PBS with 2% FBS) and 6 µL of Goat Anti-Rat IgG (H+L) antibody, FITC conjugate (SA00003-11, Cosmo Bio Co., Ltd., Tokyo, Japan; diluted 100-fold in PBS with 2% FBS) were mixed and kept at 4 ˚C under dark conditions for 30 min. After the reaction, the cells were washed three times with 1 mL of PBS (3 mL in total) and centrifuged at 250 ×g for 5 min at 4 °C to remove the supernatant. The cells were then resuspended in 1 mL of PBS, shielded from light, and stored on ice until flow cytometry analysis (EC800, SONY, Tokyo, Japan).

The fluorescence intensity of APC-H7 and FITC was measured with excitation wavelengths of 638 nm and 488 nm, and emission wavelengths of 780 nm and 525 nm, respectively. To prevent cell aggregation, the cells were dispersed using FALCON® cell strainer before measurement. The population of HT29 cells expressing both CD44 and CD44v9 was determined using the cell analyzer.

RESULTS AND DISCUSSION

Optimization of the rear constriction width for cell deformability measurements. Cell size is a critical factor affecting the residence time at the rear constriction. Before mechanotyping, the diameter of cancer cells in the suspended state was measured via microscopic observation. As shown in Figure S1, the mean diameters of 100 cancer cells were 14.8 ± 1.2 µm for HT29 cells, 15.2 ± 1.5 µm for Caco-2 cells, 15.4 ± 1.6 µm for HeLa cells, 16.4 ± 2.0 µm for MDA-MB-231 cells, and 10.8 ± 1.1 µm for Jurkat cells. Notably, these values were found to be comparable to those of several previous reports[37,38,43].

To investigate cell deformability, we prepared three different widths of the rear constriction (6, 8, and 10 µm) with a length of 30 µm. For cell size measurement at the front constriction, all of them had the same dimension, 20 µm wide and 30 µm long. All constrictions and channels had the same height (approximately 20 µm), regardless of the location. In the previous study, one of the issues that occurred at the entrance of the rear constriction was clogging of cells[37,38]. To prevent clogging and enable the smooth entry of cells, the boundary area from the middle channel to the rear constriction was tapered as shown in Figure 1(C).

Prior to the current measurement of cancer cells, we optimized the rear constriction width for cell deformability measurement to maximize the value distribution, which

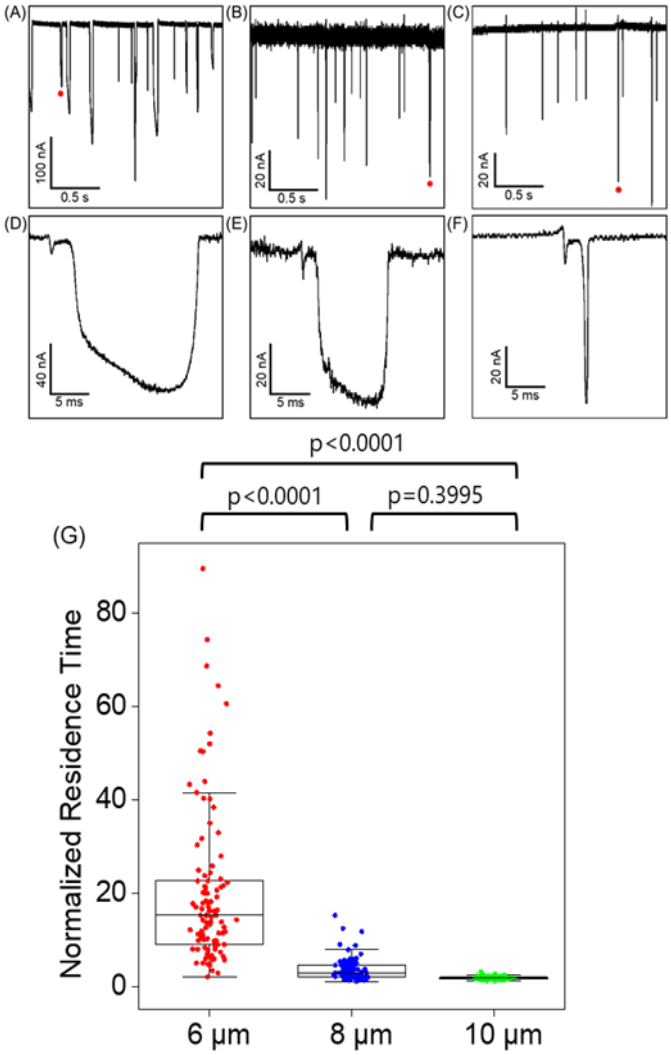

Figure 2. Optimization of the rear constriction width for cell deformability measurements. The typical current signals derived from ion current blockades by several HT29 cells migrating in the two consecutive constrictions with a width of (A) 6 µm, (B) 8 µm, and (C) 10 µm. (D, E, F) Magnified images of the typical current signals depicted by red dots in (A, B, C), respectively. The front and rear signals derived from the cell migrating in the front and the rear constrictions, respectively. The signal intensity of the front signal corresponds to the cell size. The residence time of the rear signal was used to evaluate cell deformability. (G) The normalized residence time, which is defined as the value of the residence time at the rear constriction divided by the residence time at the front constriction, was used to suppress the instability of the flow velocity. A rear constriction width of 6 µm provided the largest distribution of the normalized residence time, which indicated the highest resolution for the cell deformability measurements. The measurement conditions were as follows: RPMI at room temperature, 3 V for electrophoresis, and 3 µL/min for hydrodynamic flow.

corresponds to the resolution, using HT29 cells. To exclude the influences of unexpected hydrodynamic flow fluctuation induced by water level changes in the reservoir over time and intra- and inter-device reproducibility, the normalized residence time was defined by the following operation; the residence time at the rear constriction devided by the residence time at the front constriction which is independent of the cell

deformability. Figure 2(A)-(F) shows the raw current signals obtained by the three different width of the rear constrictions and Figure 2(G) shows the beeswarm plots of the normalized traveling time obtained by the rear constrictions. The normalized traveling time obtained for each rear constriction was 19.7 ± 16.6, 3.5 ± 2.3, and 1.8 ± 0.3 for rear constrictions with a width of 6 µm, 8 µm, and 10 µm, respectively. As a result, we concluded that the rear constriction with a width of 6 µm had the highest resolution for the mechanotyping. This design was thus employed for the subsequent experiments.

HT29 cells, Caco-2 cells, HeLa cells, and MDA-MB-231 cells (which are adherent cells) and Jurkat cells (which are floating cells) were used for cell deformability measurements. The deformation ability of these cells was measured using the current measurement method, and the normalized traveling time of each cell was compared (Fig. 3). The normalized traveling times (dimensionless quantity) of the various cells were 19.7 ± 16.6, 15.4 ± 14.3, 8.3 ± 5.6, 3.9 ± 2.7, and 1.6 ± 0.3 for HT29, Caco-2, HeLa, MDA-MB-231, and Jurkat cells, respectively. The deformability of HT29 cells and Caco-2 cells (both derived from human colon adenocarcinoma) varied more widely than that of the other three cell types. Further, the distribution of cell deformability was wider in the order of HT29, Caco-2, HeLa, and MDA-MB-231 cells. This result aligns with the order of the percentage of cancer cells with high multipotency in the cell population as revealed by the ALDH assay (discussed later).

Evaluation of the multipotency of cancer cells using a biochemical assay. Figure 3(A-D) shows the results of ALDH activity analysis of HT29, Caco-2, HeLa, and MDA-MB-231 cells. The ratio of high ALDH activity cells in the cell population was 52.2%, 24.4%, 9.1%, and 1.7% for HT29, Caco-2, HeLa, and MDA-MB-231 cells, respectively. In terms of viable cells with high FSC intensity, the variability of AldeRed™ 588-A fluorescence intensity was larger in HT29 and Caco-2 cells than in HeLa and MDA-MB-231 cells. HT29 and Caco-2 cells showed greater variation in AldeRed™ 588-A fluorescence intensity than HeLa and MDA-MB-231 cells, indicating cell population heterogeneity. Here, the intestinal epithelium is composed of absorptive epithelial cells for digestion and absorption, embryonic cells for mucus production, endocrine cells for endocrine secretion, and Paneth cells for antibacterial function, all of which are generated from differentiated intestinal epithelial stem cells[50]. Therefore, HT29 and Caco-2 cells are considered to be a heterogeneous population that has many cells with high multipotency. To verify the influence of the ALDH assay itself on cell deformability measurements, the normalized residence time of HT29 cells before and after the ALDH activity assay was measured (Figure S2). The normalized traveling time for each type of cell was 19.8±16.6 and 22.9±20.1 for the cells before and after ALDH activity assay, respectively. Although the distribution of deformability appeared slightly larger in the cell population after the ALDH assay than in cells before the assay, the ALDH assay was not found to have a significant effect on the cell deformability measurements (p=0.54142). Details of the gating processes in ALDH activity assay are shown in Figure S3-6.

CD44 and CD44 variant 9 are another type of markers for evaluating the multipotency of cancer cells. Figure 4 shows the results of flow cytometry analysis of CD44/CD44v9 double stained HT29 cells. The percentage of the double positive cells was 51.3%; this value was comparable to the previous ALDH assay results. These two biochemical data strongly support the high heterogeneity of the HT29 cell population and the multipotency of the HT29 cells.

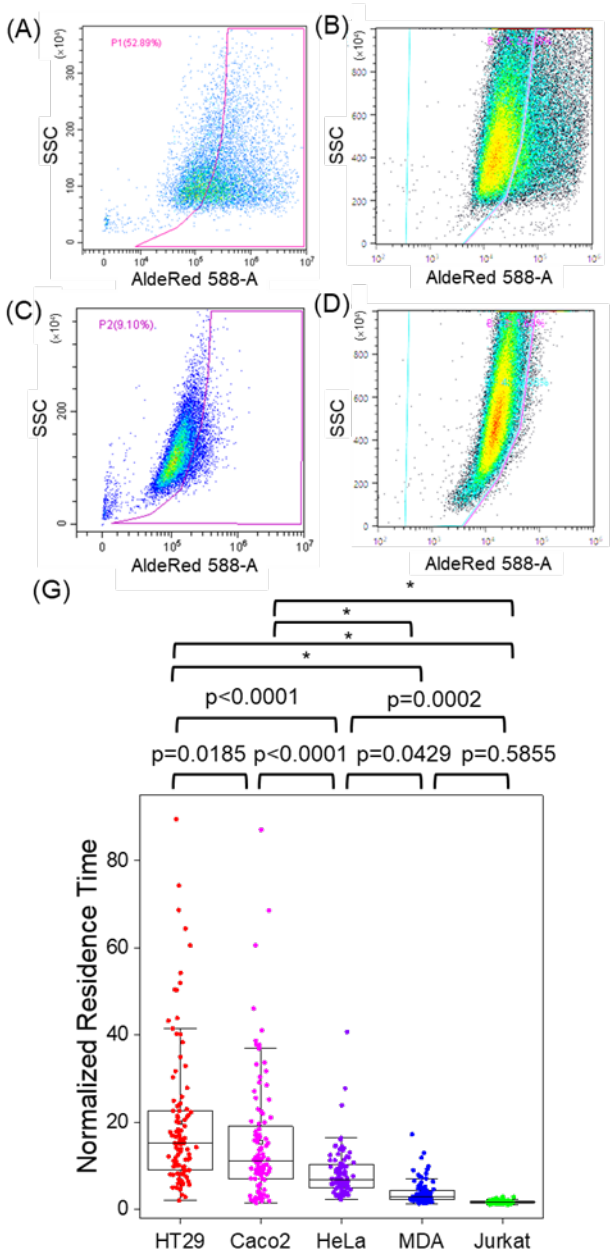

Figure 3. (A-D) ALDH activity assay using the AldeRed™ ALDH Detection Assay Kit and flow cytometry. (A) HT29 and (C) HeLa cells were measured by CytoFLEX, while (B) Caco-2 and (D) MDA-MB-231 cells were measured by SH800. (G) Mechanotyping of HT29, Caco2, HeLa, MDA-MB-231, and Jurkat cells was performed using two consecutive constrictions with rear constrictions of 6 µm. Box plots of the normalized residence time of HT29 (N= 103, red dots), Caco2 (N=100, red dots), HeLa (N=87, red dots), MDA-MB-231, and Jurkat (N=98, red dots) cells at the rear constrictions (6 µm wide). The measurement conditions were as follows: DMEM for Caco-2 and MDA-MB-231, RPMI for HT29 and Jurkat, EMEM for HeLa cells at room temperature, 3 V for electrophoresis, and 3 µL/min for hydrodynamic flow. *: p<0.0001

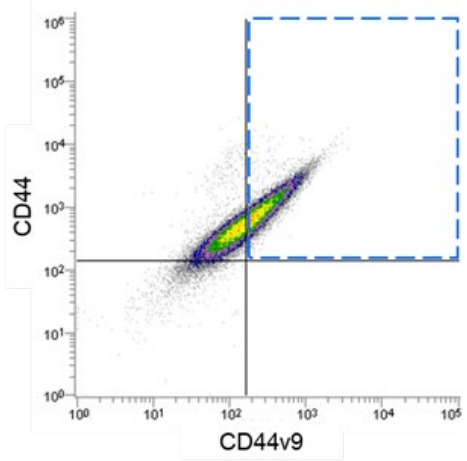

Figure 4. Flow cytometry analysis of CD44/CD44v9 double stained HT29 cells. The double positive cells indicated by a blue dashed line were 51.3%, which supports the percentage of the gated cells, and 52.2%, in the ALDH activity assay, which is shown in Fig. 3(A).

Cell deformability measurements of the sorted cells based on ALDH activity. To confirm the high heterogeneity in the HT29 cell population and the high multipotency, HT29 cells were separated and collected by FACS based on ALDH activity. Figures 5(A) and (B) show the ALDH activities of the collected low and high ALDH activity cells, respectively, at the first FACS operation. Although almost 100% of the low ALDH activity cells at the first FACS operation were detected as low ALDH activity in the second analysis, approximately half of the high ALDH activity cells at the first FACS operation were gated as high ALDH activity in the second analysis. The ALDH activity assay employed herein is dependent on the fluorescence probe that is transformed from a non-fluorogenic to fluorogenic molecule by ALDH; the produced fluorogenic molecule, AldeRed™ 588-A, remains trapped inside the cells. However, dehydrogenated AldeRed™ 588-A by ALDH might gradually diffuse out of the cells as the pKa of the carboxyl group produced by dehydrogenation of AldeRed™ 588-A may not be small enough to prevent the diffusion of all molecules out of the cell (pKa value is not disclosed). In this two consecutive FACS operation, it took a few hours to complete the second flow cytometer analysis after initiating the ALDH activity assay. As a result, natural diffusion of the fluorogenic probe out of the cells and cell damage under a severe long-time FACS operation might be reasonable causes of the fluorescent signal loss in the high ALDH activity group at the second FACS. (Figures S7, S8, Table S2).

After the first FACS operation, the deformability of each cells was measured using our mechanotyping device. As shown in Figure 5(C), the mean normalized residence time was 4.9±3.8 and 2.7±1.5 for cells with high and low ALDH activity, respectively. The long-normalized residence time of the high ALDH activity cells might support the high multipotency of HT29 cells. The distribution of the normalized residence time of the high ALDH activity cells was clearly wider than that of the low ALDH activity cells ($p<0.0001$), suggesting high heterogeneity of the HT29 cells. The partial overlap in the distribution of normalized traveling time of cells with high and low ALDH activity may be due to contamination of unintended cells during the sorting process,

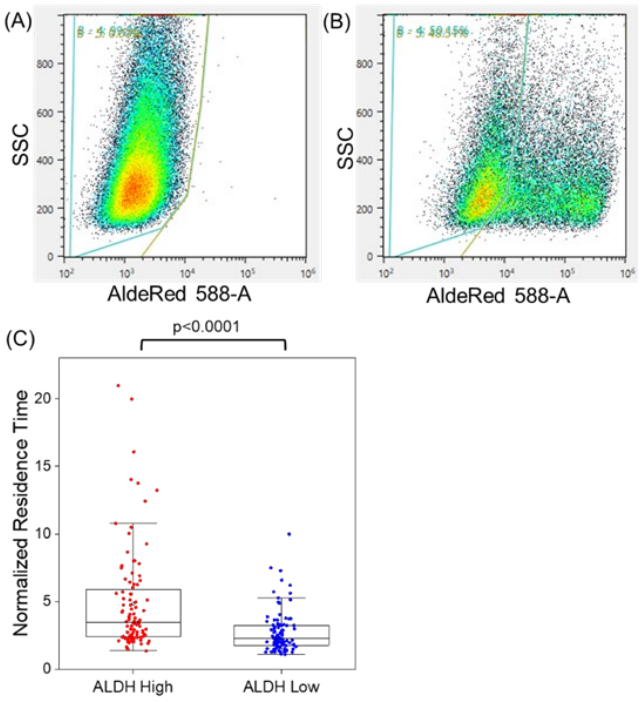

Figure 5. Flow cytometry analysis and mechanotyping results of the sorted HT29 cells by FACS based on ALDH activity. Flow cytometry analysis of (A) low and (B) high ALCH activity cells sorted by the first FACS operation. Although almost 100% of low ALDH activity cells at the first FACS operation showed low ALDH activity in the second flow cytometry analysis, 48.5% of high ALDH activity cells at the first FACS operation showed high ALDH activity in the second flow cytometry analysis. (C) Mechanotyping of the cells sorted as having high (red dots) and low (blue dots) ALDH activity at the first FACS operation. The measurement conditions were as follows: RPMI at room temperature, 3 V for electrophoresis, and 3 μL/min for hydrodynamic flow.

cell damages caused by long periods of exposure during AldeRed™ 588-A staining and FACS operation as mentioned above, and the manual gating to distinguish high and low ALDH activity at the first FACS operation. The mechanism of retardation of the normalized residence time in high ALDH activity cells is discussed later. The mean normalized residence time values depicted in Figure 5(C), namely 4.9 and 2.7, were widely different from those of the unsorted cells depicted in Figure 3(G), 19.7. The main reason may be attributed to the different cellular statuses presented in Figures 3(G) and 5(C). The mechanotyping experiments were performed nearly 1 h and 5 h after detachment of the cells from culture dishes via trypsinization, as shown in Figures 3(G) and 5(C), respectively. Additionally, the first experiment performed 1 h after detachment was executed at room temperature, whereas the latter experiment performed 5 h after detachment was executed on ice; the use of the cell samples for the following mechanotyping experiments or FACS operation was considered. The different incubation conditions established before the mechanotyping experiments may affect the surface status of cells, such as filopodia extension, and may cause the establishment of different chemical interactions between the cell surface and the rear constriction surface. Not only the cell surface molecules but also cytoskeleton structures, such as actin polymerization status, may lead to a change in the absolute values of mechanical parameters including

elasticity. Therefore, these temporal surface and internal status changes might have resulted in the achievement of different normalized residence time values depicted in Figures 3(G) and 5(C); however, they were not critical to cell life.

Although ALDH activity has been reported as a marker for normal colonic stem cells and colorectal CSCs for almost a decade[34], little is known about the fate of these cells and their relationship to colonic stem-like cells defined by several markers. Although available biochemical data remain limited for assigning colonic stem-like cells, the application of retinoic acid to HT29 cells was reported to be linked with ALDH1 expression level, which suggested its potential as a promising target for therapeutics[44]. Moise et al. reported that retinoic acid signaling facilitates the cytoskeletal rearrangement required for the epicardial-to-mesenchymal transition of epicardial cells[45]. In their study, the Ras homolog gene family member A (RhoA) pathway was found to be required for the morphologic changes induced by retinoic acid in epicardial cells. In HT29 cells, RhoA was found to induce actomyosin contraction at the apical cortex[46]. Currently, the role of retinoic acid in HT29 cells remains unclear; however, the above results might support the finding that a high expression level of ALDH1 is linked with cytoskeletal changes through the RhoA pathway, which could cause direct changes in the mechanical phenotype through the cytoskeleton.

Altogether, our findings revealed the potential of performing a single cell mechanotyping using microfluidic devices to identify CSCs in heterogeneous cancer cell population corroborated by existing biochemical markers. Further studies comprehensively analyzing gene expression and metabolites levels will be necessary to gain a complete understanding of how changes in molecular constituents affect the mechanical phenotype. Such studies will also contribute to the establishment of biophysical markers that will aid in the development of a non-invasive and non-label single cell diagnostic technique, not only for use in fundamental research but also in clinical diagnosis.

CONCLUSION

Herein, consecutive constrictions and an ionic current sensing system were applied as a label-free and non-destructive diagnosis technique to identify CSCs in a large population of cells based on cell sizing and deformability measurements at a single cell level with a moderate throughput, ~10 cells/s. A rear constriction with a width of 6 μm enabled highly resolved distinction of the multipotency of the cancer cells, HT29, from other cell types, such as Caco-2, HeLa, MDA-MB-231, and Jurkat, based on the residence time when passing through the rear constriction. The large heterogeneity among the cell population of HT29 was also confirmed via a biochemical assay, ALDH activity, and CD44s expression level, which are known to be parameters of the multipotency of cells. Although the mechanism whereby changes in the above biochemical parameters affect the mechanical property of cells remains unclear (i.e., a high expression level of ALDH1 was previously found to lead to cytoskeletal changes through the RhoA pathway), changes in several biochemical parameters in CSCs might cause quantitative or qualitative changes in the cytoskeletal structures, which is directly linked with cell deformability. Therefore, the proposed CSCs assay is expected to serve as an initial screening method for CSCs before the performance of destructive detailed diagnoses, such as immunochemistry and gene expression analysis.

ASSOCIATED CONTENT

Supporting Information

Supporting Information is available free of charge on the ACS Publications website.

Changes in the deformability of HT29 cells before and after the ALDH activity assay, flow cytometry analysis of HT29 cells with and without a selective inhibitor of ALDH (DEAB), and electric conductivity of the buffer and medium used in this study (PDF).

AUTHOR INFORMATION

Corresponding Author

Noritada Kaji - Department of Applied Chemistry, Graduate School of Engineering, Kyushu University, 744 Motooka, Nishi-ku, Fukuoka 819-0395, Japan; orcid.org/0000-0002-9828-873X; Phone: +81-92-802-2883; Email: kaji@cstf.kyushu-u.ac.jp

Author Contributions

All authors have approved the final version of the manuscript.

Notes

The authors declare no competing financial interest.

ACKNOWLEDGMENT

The authors wish to thank Prof. Yoshiki Katayama and Mr. Keiichiro Ono for their technical assistant in flow cytometry analysis using CytoFLEX S (Beckman Coulter) as well as Dr. Yuki Okugawa for her technical assistant in FACS operation using SH800 (Sony). This work was partially supported by JST/PRESTO [grant number JPMJPR16F4], Grant-in-Aid for Scientific Research (B) [21H01966], Grant-in-Aid for Scientific Research on Innovative Areas (Research in a proposed research area) [20H04714], Fund for the Promotion of Joint International Research (Fostering Joint International Research (B)) (19KK0140), a research grant from the Shimadzu Science Foundation, a research grant from Toyota Riken Scholar, and a research grant from Casio Science Promotion Foundation.

References

(1) Di Carlo, D., A Mechanical Biomarker of Cell State in Medicine. *Journal of Laboratory Automation* **2012,** *17* (1), 32-42.

(2) Otto, O.; Rosendahl, P.; Mietke, A.; Golfier, S.; Herold, C.; Klaue, D.; Girardo, S.; Pagliara, S.; Ekpenyong, A.; Jacobi, A.; Wobus, M.; Töpfner, N.; Keyser, U. F.; Mansfeld, J.; Fischer-Friedrich, E.; Guck, J., Real-time deformability cytometry: on-the-fly cell mechanical phenotyping. *Nature Methods* **2015,** *12* (3), 199-202.

(3) Swaminathan, V.; Mythreye, K.; O'Brien, E. T.; Berchuck, A.; Blobe, G. C.; Superfine, R., Mechanical Stiffness Grades Metastatic Potential in Patient Tumor Cells and in Cancer Cell Lines. *Cancer Research* **2011,** *71* (15), 5075-5080.

(4) Byun, S.; Son, S.; Amodei, D.; Cermak, N.; Shaw, J.; Kang, J. H.; Hecht, V. C.; Winslow, M. M.; Jacks, T.; Mallick, P.; Manalis, S. R., Characterizing deformability and surface friction of cancer cells. *Proceedings of the National Academy of Sciences* **2013,** *110* (19), 7580-7585.

(5) Gossett, D. R.; Tse, H. T. K.; Lee, S. A.; Ying, Y.; Lindgren, A. G.; Yang, O. O.; Rao, J.; Clark, A. T.; Di Carlo, D., Hydrodynamic stretching of single cells for large population mechanical phenotyping. *Proceedings of the National Academy of Sciences* **2012,** *109* (20), 7630-7635.

(6) Urbanska, M.; Winzi, M.; Neumann, K.; Abuhattum, S.; Rosendahl, P.; Müller, P.; Taubenberger, A.; Anastassiadis, K.; Guck, J., Single-cell mechanical phenotype is an intrinsic marker of

reprogramming and differentiation along the mouse neural lineage. *Development* **2017,** *144* (23), 4313-4321.

(7) Lin, J.; Kim, D.; Tse, H. T.; Tseng, P.; Peng, L.; Dhar, M.; Karumbayaram, S.; Di Carlo, D., High-throughput physical phenotyping of cell differentiation. *Microsystems & Nanoengineering* **2017,** *3* (1), 17013.

(8) Rosendahl, P.; Plak, K.; Jacobi, A.; Kraeter, M.; Toepfner, N.; Otto, O.; Herold, C.; Winzi, M.; Herbig, M.; Ge, Y.; Girardo, S.; Wagner, K.; Baum, B.; Guck, J., Real-time fluorescence and deformability cytometry. *Nature Methods* **2018,** *15* (5), 355-358.

(9) Rosenbluth, M. J.; Lam, W. A.; Fletcher, D. A., Analyzing cell mechanics in hematologic diseases with microfluidic biophysical flow cytometry. *Lab on a Chip* **2008,** *8* (7), 1062-1070.

(10) Bufi, N.; Saitakis, M.; Dogniaux, S.; Buschinger, O.; Bohineust, A.; Richert, A.; Maurin, M.; Hivroz, C.; Asnacios, A., Human Primary Immune Cells Exhibit Distinct Mechanical Properties that Are Modified by Inflammation. *Biophys. J.* **2015,** *108* (9), 2181-2190.

(11) Hochmuth, R. M., Micropipette aspiration of living cells. *Journal of Biomechanics* **2000,** *33* (1), 15-22.

(12) Gifford, S. C.; Frank, M. G.; Derganc, J.; Gabel, C.; Austin, R. H.; Yoshida, T.; Bitensky, M. W., Parallel microchannel-based measurements of individual erythrocyte areas and volumes. *Biophys. J.* **2003,** *84* (1), 623-633.

(13) Gill, N. K.; Ly, C.; Nyberg, K. D.; Lee, L.; Qi, D.; Tofig, B.; Reis-Sobreiro, M.; Dorigo, O.; Rao, J.; Wiedemeyer, R.; Karlan, B.; Lawrenson, K.; Freeman, M. R.; Damoiseaux, R.; Rowat, A. C., A scalable filtration method for high throughput screening based on cell deformability. *Lab on a Chip* **2019,** *19* (2), 343-357.

(14) Lautenschläger, F.; Paschke, S.; Schinkinger, S.; Bruel, A.; Beil, M.; Guck, J., The regulatory role of cell mechanics for migration of differentiating myeloid cells. *Proceedings of the National Academy of Sciences* **2009,** *106* (37), 15696-15701.

(15) Rotsch, C.; Jacobson, K.; Radmacher, M., Dimensional and mechanical dynamics of active and stable edges in motile fibroblasts investigated by using atomic force microscopy. *Proceedings of the National Academy of Sciences* **1999,** *96* (3), 921-926.

(16) Thoumine, O.; Ott, A., Time scale dependent viscoelastic and contractile regimes in fibroblasts probed by microplate manipulation. *J. Cell Sci.* **1997,** *110* (17), 2109-2116.

(17) Bausch, A. R.; Möller, W.; Sackmann, E., Measurement of local viscoelasticity and forces in living cells by magnetic tweezers. *Biophys. J.* **1999,** *76* (1 Pt 1), 573-579.

(18) Urbanska, M.; Muñoz, H. E.; Shaw Bagnall, J.; Otto, O.; Manalis, S. R.; Di Carlo, D.; Guck, J., A comparison of microfluidic methods for high-throughput cell deformability measurements. *Nat Methods* **2020,** *17* (6), 587-593.

(19) Lee, W. C.; Shi, H.; Poon, Z.; Nyan, L. M.; Kaushik, T.; Shivashankar, G. V.; Chan, J. K. Y.; Lim, C. T.; Han, J.; Van Vliet, K. J., Multivariate biophysical markers predictive of mesenchymal stromal cell multipotency. *Proceedings of the National Academy of Sciences* **2014,** *111* (42), E4409-E4418.

(20) Lapidot, T.; Sirard, C.; Vormoor, J.; Murdoch, B.; Hoang, T.; Caceres-Cortes, J.; Minden, M.; Paterson, B.; Caligiuri, M. A.; Dick, J. E., A cell initiating human acute myeloid leukaemia after transplantation into SCID mice. *Nature* **1994,** *367* (6464), 645-648.

(21) Bonnet, D.; Dick, J. E., Human acute myeloid leukemia is organized as a hierarchy that originates from a primitive hematopoietic cell. *Nature Medicine* **1997,** *3* (7), 730-737.

(22) Al-Hajj, M.; Wicha, M. S.; Benito-Hernandez, A.; Morrison, S. J.; Clarke, M. F., Prospective identification of tumorigenic breast cancer cells. *Proceedings of the National Academy of Sciences* **2003,** *100* (7), 3983-3988.

(23) Collins, A. T.; Berry, P. A.; Hyde, C.; Stower, M. J.; Maitland, N. J., Prospective Identification of Tumorigenic Prostate Cancer Stem Cells. *Cancer Research* **2005,** *65* (23), 10946-10951.

(24) Hermann, P. C.; Huber, S. L.; Herrler, T.; Aicher, A.; Ellwart, J. W.; Guba, M.; Bruns, C. J.; Heeschen, C., Distinct Populations of Cancer Stem Cells Determine Tumor Growth and Metastatic Activity in Human Pancreatic Cancer. *Cell Stem Cell* **2007,** *1* (3), 313-323.

(25) O'Brien, C. A.; Pollett, A.; Gallinger, S.; Dick, J. E., A human colon cancer cell capable of initiating tumour growth in immunodeficient mice. *Nature* **2007,** *445* (7123), 106-110.

(26) Curley, M. D.; Therrien, V. A.; Cummings, C. L.; Sergent, P. A.; Koulouris, C. R.; Friel, A. M.; Roberts, D. J.; Seiden, M. V.; Scadden, D. T.; Rueda, B. R.; Foster, R., CD133 Expression Defines a Tumor Initiating Cell Population in Primary Human Ovarian Cancer. *STEM CELLS* **2009,** *27* (12), 2875-2883.

(27) Suwannakul, N.; Ma, N.; Thanan, R.; Pinlaor, S.; Ungarreevittaya, P.; Midorikawa, K.; Hiraku, Y.; Oikawa, S.; Kawanishi, S.; Murata, M., Overexpression of CD44 Variant 9: A Novel Cancer Stem Cell Marker in Human Cholangiocarcinoma in Relation to Inflammation. *Mediators of Inflammation* **2018,** *2018*, 4867234.

(28) Ishimoto, T.; Nagano, O.; Yae, T.; Tamada, M.; Motohara, T.; Oshima, H.; Oshima, M.; Ikeda, T.; Asaba, R.; Yagi, H.; Masuko, T.; Shimizu, T.; Ishikawa, T.; Kai, K.; Takahashi, E.; Imamura, Y.; Baba, Y.; Ohmura, M.; Suematsu, M.; Baba, H.; Saya, H., CD44 variant regulates redox status in cancer cells by stabilizing the xCT subunit of system xc(-) and thereby promotes tumor growth. *Cancer Cell* **2011,** *19* (3), 387-400.

(29) Mima, K.; Okabe, H.; Ishimoto, T.; Hayashi, H.; Nakagawa, S.; Kuroki, H.; Watanabe, M.; Beppu, T.; Tamada, M.; Nagano, O.; Saya, H.; Baba, H., CD44s regulates the TGF-beta-mediated mesenchymal phenotype and is associated with poor prognosis in patients with hepatocellular carcinoma. *Cancer Res* **2012,** *72* (13), 3414-23.

(30) Morrin, M.; Delaney, P. V., CD44v6 is not relevant in colorectal tumour progression. *Int J Colorectal Dis* **2002,** *17* (1), 30-6.

(31) Coppola, D.; Hyacinthe, M.; Fu, L.; Cantor, A. B.; Karl, R.; Marcet, J.; Cooper, D. L.; Nicosia, S. V.; Cooper, H. S., CD44V6 expression in human colorectal carcinoma. *Hum Pathol* **1998,** *29* (6), 627-35.

(32) Shuang, Z. Y.; Wu, W. C.; Xu, J.; Lin, G.; Liu, Y. C.; Lao, X. M.; Zheng, L.; Li, S., Transforming growth factor-beta1-induced epithelial-mesenchymal transition generates ALDH-positive cells with stem cell properties in cholangiocarcinoma. *Cancer Lett* **2014,** *354* (2), 320-8.

(33) Lingala, S.; Cui, Y. Y.; Chen, X.; Ruebner, B. H.; Qian, X. F.; Zern, M. A.; Wu, J., Immunohistochemical staining of cancer stem cell markers in hepatocellular carcinoma. *Exp Mol Pathol* **2010,** *89* (1), 27-35.

(34) Huang, E. H.; Hynes, M. J.; Zhang, T.; Ginestier, C.; Dontu, G.; Appelman, H.; Fields, J. Z.; Wicha, M. S.; Boman, B. M., Aldehyde Dehydrogenase 1 Is a Marker for Normal and Malignant Human Colonic Stem Cells (SC) and Tracks SC Overpopulation during Colon Tumorigenesis. *Cancer Research* **2009,** *69* (8), 3382-3389.

(35) Chu, P.; Clanton, D. J.; Snipas, T. S.; Lee, J.; Mitchell, E.; Nguyen, M. L.; Hare, E.; Peach, R. J., Characterization of a subpopulation of colon cancer cells with stem cell-like properties. *International Journal of Cancer* **2009,** *124* (6), 1312-1321.

(36) Khorrami, S.; Hosseini, A. Z.; Mowla, S. J.; Malekzadeh, R., Verification of ALDH Activity as a Biomarker in Colon Cancer Stem Cells-Derived HT-29 Cell Line. *Iranian Journal of Cancer Prevention* **2015,** *8* (5).

(37) Sano, M.; Kaji, N.; Rowat, A. C.; Yasaki, H.; Shao, L.; Odaka, H.; Yasui, T.; Higashiyama, T.; Baba, Y., Microfluidic Mechanotyping of a Single Cell with Two Consecutive Constrictions of Different Sizes and an Electrical Detection System. *Anal. Chem.* **2019,** *91* (20), 12890-12899.

(38) Suzuki, T.; Kaji, N.; Yasaki, H.; Yasui, T.; Baba, Y., Mechanical Low-Pass Filtering of Cells for Detection of Circulating Tumor Cells in Whole Blood. *Anal. Chem.* **2020,** *92* (3), 2483-2491.

(39) Yasaki, H.; Shimada, T.; Yasui, T.; Yanagida, T.; Kaji, N.; Kanai, M.; Nagashima, K.; Kawai, T.; Baba, Y., Robust Ionic Current Sensor for Bacterial Cell Size Detection. *ACS Sens* **2018,** *3* (3), 574-579.

(40) Yasaki, H.; Yasui, T.; Yanagida, T.; Kaji, N.; Kanai, M.; Nagashima, K.; Kawai, T.; Baba, Y., Substantial Expansion of Detectable Size Range in Ionic Current Sensing through Pores by Using a Microfluidic Bridge Circuit. *J. Am. Chem. Soc.* **2017,** *139* (40), 14137-14142.

(41) Yasaki, H.; Yasui, T.; Yanagida, T.; Kaji, N.; Kanai, M.; Nagashima, K.; Kawai, T.; Baba, Y., Effect of Channel Geometry on Ionic Current Signal of a Bridge Circuit Based Microfluidic Channel. *Chem. Lett.* **2018,** *47* (3), 350-353.

(42) Yasaki, H.; Yasui, T.; Yanagida, T.; Kaji, N.; Kanai, M.; Nagashima, K.; Kawai, T.; Baba, Y., A real-time simultaneous measurement on a microfluidic device for individual bacteria discrimination. *Sensors and Actuators B-Chemical* **2018,** *260*, 746-752.

(43) Valencia-Cruz, G.; Shabala, L.; Delgado-Enciso, I.; Shabala, S.; Bonales-Alatorre, E.; Pottosin, I. I.; Dobrovinskaya, O. R., Kbg and Kv1.3 channels mediate potassium efflux in the early phase of apoptosis in Jurkat T lymphocytes. *American Journal of Physiology-Cell Physiology* **2009,** *297* (6), C1544-C1553.

(44) Bhatlekar, S.; Viswanathan, V.; Fields, J. Z.; Boman, B. M., Overexpression of HOXA4 and HOXA9 genes promotes self-renewal and contributes to colon cancer stem cell overpopulation. *J. Cell. Physiol.* **2018,** *233* (2), 727-735.

(45) Wang, S. Y.; Yu, J. S.; Jones, J. W.; Pierzchalski, K.; Kane, M. A.; Trainor, P. A.; Xavier-Neto, J.; Moise, A. R., Retinoic acid signaling promotes the cytoskeletal rearrangement of embryonic epicardial cells. *FASEB J.* **2018,** *32* (7), 3765-3781.

(46) Ito, S.; Okuda, S.; Abe, M.; Fujimoto, M.; Onuki, T.; Nishimura, T.; Takeichi, M., Induced cortical tension restores functional junctions in adhesion-defective carcinoma cells. *Nature Communications* **2017,** *8* (1), 1834.

For Table of Contents Only